AD_____

Award Number:

W81XWH-08-2-0004

TITLE:

"Targeted Delivery of Carbon Nanotubes to Cancer Cells"

PRINCIPAL INVESTIGATOR:

Ellen Vitetta, PhD

CONTRACTING ORGANIZATION:

University of Texas Southwestern Medical Center at Dallas
Dallas, Texas 75390

REPORT DATE:

January 2009

TYPE OF REPORT:

Annual Report

PREPARED FOR: **U.S. Army Medical Research and Materiel Command**
Fort Detrick, Maryland 21702-5012

DISTRIBUTION STATEMENT:

Approved for public release; distribution unlimited

REPORT DOCUMENTATION PAGE

Form Approved
OMB No. 0704-0188

1. REPORT DATE *(DD-MM-YYYY)*	2. REPORT TYPE	3. DATES COVERED *(From - To)*
01-01-2009	Annual	14 Dec 2007 – 13 Dec 2008

4. TITLE AND SUBTITLE

Targeted Delivery of Carbon Nanotubes to Cancer Cells

5a. CONTRACT NUMBER

5b. GRANT NUMBER
W81XWH-08-2-0004

5c. PROGRAM ELEMENT NUMBER

6. AUTHOR(S)

Ellen Vitetta, PhD

5d. PROJECT NUMBER

5e. TASK NUMBER

5f. WORK UNIT NUMBER

7. PERFORMING ORGANIZATION NAME(S) AND ADDRESS(ES)

University of Texas Southwestern Medic
Center at Dallas

Dallas, Texas 75390

8. PERFORMING ORGANIZATION REPORT NUMBER

9. SPONSORING / MONITORING AGENCY NAME(S) AND ADDRESS(ES)

U.S. Army Medical Research
and Materiel Command
Fort Detrick, Maryland 21702-5012

10. SPONSOR/MONITOR'S ACRONYM(S)

11. SPONSOR/MONITOR'S REPORT NUMBER(S)

12. DISTRIBUTION / AVAILABILITY STATEMENT

Approved for public release; distribution unlimited.

13. SUPPLEMENTARY NOTES

14. ABSTRACT

Single-walled carbon nanotubes (CNTs) convert absorbed near infrared (NIR) light into heat, which can thermally ablate cells that have bound the CNTs. CNTs coupled to monoclonal antibodies (MAbs) may specifically target and kill cells by non-invasive exposure to near infrared (NIR) light. Here, we describe the preparation of conjugates in which CNTs are either non-covalently or covalently conjugated to the MAbs against human CD22 or CD25. In the first approach, biotinylated polar lipids were used to prepare stable, biocompatible, non-cytotoxic CNT suspensions that were then attached to one of the two different Neutralite Avidin (NA)-derivatized MAbs.. In the second approach the two MAbs were covalently coupled to carboxylated CNTs. The specificity of the binding and killing of the target cells by both types of MAb-CNTs was demonstrated by using CD22+CD25- Daudi cells, CD22-CD25+ phytohemagglutinin (PHA)-activated normal human peripheral blood mononuclear cells (PBMCs). We also demonstrate that the conjugates were stable and active following incubation with mouse serum.

15. SUBJECT TERMS

carbon nanotubes, tumor targeting, monoclonal antibody

16. SECURITY CLASSIFICATION OF:			17. LIMITATION OF ABSTRACT	18. NUMBER OF PAGES	19a. NAME OF RESPONSIBLE PERSON USAMRMC
a. REPORT	b. ABSTRACT	c. THIS PAGE			19b. TELEPHONE NUMBER *(include area code)*
U	U	U	UU	17	

Standard Form 298 (Rev. 8-98)
Prescribed by ANSI Std. Z39.18

Table of Contents

Page

INTRODUCTION

The objective of this project is to target carbon nanotubes (CNTs) to tumor cells and thermally ablate the cells by exploiting the ability of CNTs to absorb energy in regions of the electromagnetic spectrum that penetrate tissue and convert the energy to heat.

BODY

Task 1. To attach MAb to CNTs.

We used 2 strategies to attach targeting MAbs to CNTs: noncovalent and covalent.

I. Non-Covalent Attachment of MAbs to CNTs Adsorbed with Biotinylated Fatty Acid Conjugates
This is a 2-step procedure that involves CNTs dispersion with biotinylated polar lipids, preparation of neutravidin-derivatized targeting MAb followed by their coupling.

CNT Dispersion by Biotinylated Polar Lipids**.** Degassed ultrapure deionized (DI) water was used for all solutions. Single-walled CNTs (HiPco) (0.3 mg) were suspended in 1 ml of 166 μM 1, 2-distearoyl-sn-glycero-3-phosphoethanolamine-N-[biotinyl(polyethylene glycol) 2000] (DSPE-PEG(2000)-biotin). The mixture was sonicated with a 2 mm probe tip connected to a Branson Sonifier 250 (VWR, West Chester, PA) for 10 min at a power level of 10 W, with the sample immersed in an ice water bath. To remove excess DSPE-PEG-biotin, samples were washed twice in distilled (DI) water by centrifugation for 15 min at 90,000 *x g* at 4°C. The supernatant was discarded, the pellet was resuspended in 1 ml of DI water, and the procedure repeated. The samples were then centrifuged two times for 10 min at 16,000 *x g* at room temperature and the upper 50% of the supernatant containing the biotinylated CNTs (B-CNTs) was recovered. In order to obtain more concentrated samples, the B-CNT suspension was centrifuged for 60 min at 16,000 *x g* at 4°C, the supernatant discarded, and the pellet was resuspended in 0.2 ml of DI water.

The resulting B-CNT suspension contained 0.06 mg CNT/ml and ≤ 3 parts per million metals, as determined by thermal gravimetric analysis (TGA). The dispersions were stable and did not aggregate at room temperature for over 120 days. Atomic force microscopy (AFM) analysis demonstrated that the suspension was free of non-tubular carbon structures and that the CNTs were either individually dispersed or in small bundles. The lengths of the CNTs ranged from 0.2 to 1.4 μm with an average of 0.59 μm (**Fig. 1a**). Analysis by transmission electron microscopy (TEM) of the B-CNT samples probed with gold-labeled goat anti-biotin demonstrated that biotin was distributed along the entire surface of the B-CNT (**Fig. 1b**). The biotin content of the B-CNT dispersion was determined using a competitive enzyme-linked immunosorbent assay (ELISA). This was accomplished by adding dilutions of the B-CNT dispersion to biotin-horseradish peroxidase (HRP) and plating them onto neutravidin (NA)-coated plates. The amount of HRP-labeled biotin was detected by the development of color in the presence of the 2, 2'-azino-bis(3-ethylbenzothiazoline-6-sulfonic acid) (ABTS) substrate. Using this assay, we found that the content of biotin was 0.02 mmol per gram of B-CNT. The UV-Vis-NIR spectra of the B-CNTs confirmed the quality of these dispersions with the presence of electronic transitions between van Hove singularities suggesting that the optical properties of the CNTs were maintained following the adsorption of DSPE-PEG-biotin (**Fig. 1c**). The Raman spectra of the B-CNTs showed a number of well characterized CNT resonances such as the tangential (G-band) peak at 1590 cm^{-1}, confirming the presence of CNTs in the sample (**Fig. 1d**).

Preparation of MAb-NA Conjugates**.** To couple the B-CNTs to MAbs, we used a modified protocol (33). Briefly, 10 mg of IgG anti-CD22 (RFB4) or anti-CD25 (RFT5) in 1 ml of 0.15 M borate buffer, 0.1 mM EDTA, pH 8.5 were thiolated by incubation for 1 h at room temperature with a 20:1 molar excess of Traut's reagent. After incubation, the reaction was quenched with 0.1 M glycine. In parallel, 10 mg of NA dissolved in 1 ml of 0.01 M PBS, 0.1 mM EDTA, pH 7.4, were activated by 30 min incubation at room temperature using a 6:1 molar excess of MBS. The unreacted Traut's reagent and MBS were removed by gel-filtration on Sephadex G-25 columns in 0.01 M PBS, 0.1 mM EDTA, pH 7.4. The thiolated MAb was conjugated to the activated NA at a molar ratio of 1:2 for 2 h at room temperature with gentle shaking. The resultant conjugate was purified by gel-filtration on a Sephacryl S-300 HR column (GE Healthcare) using 0.1 M PBS, 0.05% Tween-20, pH 7.4 (**Fig. 2a**). The protein concentration in the

purified conjugate was quantified using the bicinchoninic acid (BCA) protein assay (Pierce Endogen). The size and integrity of the conjugate was analyzed by western blot. The samples were electrophoresed on a 7.5% non-denaturing polyacrylamide gel and transferred to polyvinylidene difluoride membranes (Bio-Rad Laboratories, Hercules, CA), probed with HRP-labeled sheep anti-mouse IgG, and visualized using an enhanced chemiluminescence system (GE Healthcare) (**Fig. 2b**).

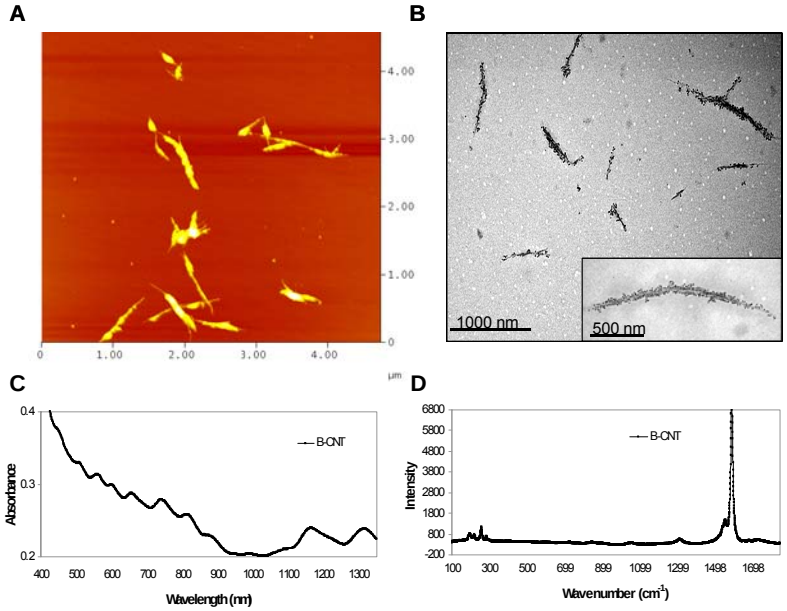

Figure 1. Analysis of the dispersed CNTs. The CNTs were dispersed by sonication in the presence of DSPE-PEG-biotin then washed/centrifuged twice at 90,000*xg* and twice at 16,000*xg*. The last supernatant that contains the dispersed CNTs was collected. **A.** Atomic force microscopy (AFM) indicates a good dispersion of the CNTs. **B.** TEM images of B-CNTs show uniform distribution of biotin after immunodetection with gold-labeled anti-biotin. **C.** UV/Vis spectra of CNT dispersions show multiple well-defined peaks compared to the spectra of the initial bundled CNTs. **D.** Raman spectra indicates a strong G band signature (1590 cm^{-1}), a diagnostic for CNTs, and a very low D band signal (1350 cm^{-1}), indicative of amorphic carbon structures.

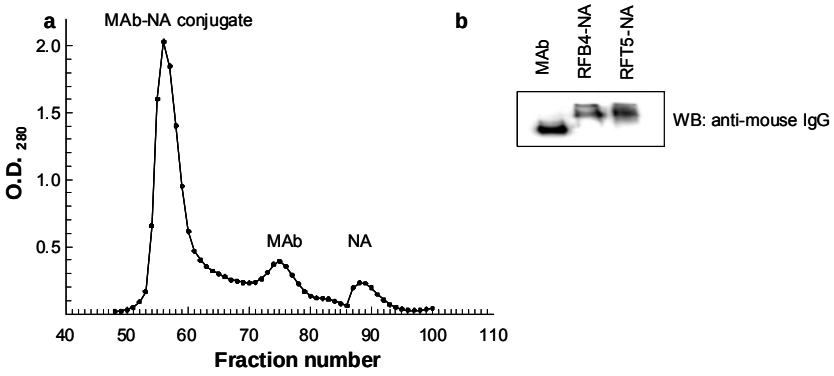

Figure 2. Analysis of MAb-NA conjugates. *(a)* A typical chromatographic separation of RFB4-NA from unconjugated RFB4 and NA using a Sephacryl S-300 HR column. Fractions of the first peak containing the RFB4-NA conjugate were pooled and concentrated. *Inset:* Purified RFB4-NA, RFT5-NA or MAb were electrophoresed under non-denaturing conditions on a 7.5% polyacrylamide gel and immunoblotted with HRP-labeled sheep anti-mouse IgG. Data in *a* and *b* are representative of at least three independent experiments.

To determine whether B-CNTs were inherently cytotoxic (in the absence of NIR), cells from the IgM^+ $CD22^+CD25^-$ Burkitt's lymphoma cell line Daudi, were incubated for 24 h with up to the highest amount of B-CNTs used in the binding and killing assays (3.6 μg). No toxicity was observed using a [^{3}H]-Thymidine incorporation assay (data not shown).

Preparation, purification, and analysis of noncovalent MAb-CNT complexes. Fresh MAb-CNTs were prepared immediately before use by mixing B-CNT with MAb-NA in a 1:2 (w/w) ratio. The mixture was placed on a rocker for 35 min at room temperature and vortexed gently every 5 min. After coupling, the mixture was centrifuged for 5 min at 16,000 *x g* at 4°C, the supernatant containing unreacted MAb-NA was discarded, and the pellet was resuspended in 40 μl of PBS for every 3.6 μg B-CNT and used immediately.

II. Covalent Attachment of MAbs to carboxyl-functionalized CNTs

In this approach we used carboxyl-functionalized CNTs to which we covalently coupled targeting MAbs.

Carboxyl-functionalized CNTs (0.5 mg) were dispersed in 1 ml of 0.1 M 2-[*N*-morpholino]ethane sulfonic acid (MES) buffer, pH 4.5 with 0.2% Tween-20 (activation buffer) by sonication with a 2 mm probe tip connected to a Branson Sonifier 250 (VWR, West Chester, PA) for 5 min at a power level of 10 W, with the sample immersed in ice. The mixture was then centrifuged at 16,000 x *g* for 15 min to remove undispersed material. The supernatant containing the dispersed CNTs was recovered. The carboxyl groups on the CNTs were activated by incubation for 30 min at room temperature with 2 mM EDC and 5 mM NHS. The excess reagents were removed by centrifugation in Amicon Ultra-4 centrifugal filter unit (Millipore, MA) and rinsed with binding buffer (0.1 M PBS, pH 7.2 with 0.2% Tween-20). The activated CNTs were recovered in 1 ml binding buffer and reacted with 10 mg IgG anti-CD22 (RFB4) or IgG anti-CD25 (RFT5) MAbs for 2 h at room temperature by gentle rocking. The control for covalent coupling was a mixture of MAbs and non-activated, carboxyl-functionalized CNTs. The unreacted MAbs were removed by centrifugation at 16,000 x *g* for 30 min. The supernatant containing unreacted MAb was discarded, and the pellet was resuspended and washed twice in 1 ml of phosphate buffered saline (PBS) buffer (10 mM, pH 7.4). After each wash, the CNTs were briefly sonicated for 10 seconds at a power level of 10 W. The amount of CNT-bound MAbs was quantified using the bicinchoninic acid (BCA) protein assay (Pierce Endogen) and the CNT concentration was determined by the absorbance at 808 nm using a DU-730 Beckman-Coulter UV/Vis spectrophotometer (Fullerton, CA). In order to directly visualize the binding of MAb-CNTs to target cells, CNTs were conjugated to both MAb and enhanced green fluorescent protein (EGFP). For the coupling reaction 10 mg MAb and 100 μg EGFP were reacted with activated CNTs as mentioned above.

Relationship to the work of others: The first critical challenge in the field of targeted CNTs is to create soluble and stable CNTs that retain both the specificity of the targeting moiety and the thermal activity of the CNTs even in serum at physiological temperatures. Our strategies involved noncovalent attachment of targeting moiety consisting of MAb-NAs to the dispersed biotinylated CNTs (non-covalent MAb-CNTs) and chemical link of the targeting MAb to carboxyl-functionalized CNTs (covalent MAb-CNTs). The first approach gave us the flexibility to "assemble" the targeted CNTs using any tumor-binding MAb. Also, the strategy of generating dispersed CNTs using biotinylated polar lipids has the advantage of preventing subsequent chemical treatments that remove the adsorbed polar lipids and/or destroy the optical properties of CNTs. Of equal importance is the specificity of the targeting strategy. Thus, previous studies have demonstrated that folic acid -coated CNTs could be targeted to folate receptor (FR)-positive cells and that NIR light killed the cells (1). Although FR-negative cells were used as a control, CNTs coated with an irrelevant control peptide or ligand were not. Another published approach for targeting CNTs to cells was to attach MAbs by direct adsorbtion that can be used in photothermal therapy (2) or imaging (3). However, attachment of MAbs by direct adsorption on CNTs involves a potential loss of the targeting function of the MAbs and indeed in the study cited, specificity controls were not reported, and cell viability studies showed 50% collateral damage by the irrelevant MAb-CNT control following exposure to NIR light (2).

The potential cytotoxicity of CNTs has been of concern for their use for therapy. One of the major challenges is to minimize their nonspecific interaction with serum proteins and/or cells and tissues and increase their half-life in the circulation. In previous reports, this was achieved by coating CNTs with biocompatible compounds, such as hydrophilic uncharged polymers including poly-(ethylene glycol) (PEG). Pharmacokinetics studies with such coated CNTs have demonstrated that CNTs dispersed by different noncovalent procedures are not toxic to mice (4-6).

Moreover, carboxyl functionalization, as we used in our second approach, increases their solubility and decreases their cytotoxicity (7). In our study, the viability of cells cultured with non-binding MAb-CNTs was indistinguishable from that of cells grown in the absence of CNTs.

Task 2. **To purify the MAb-CNT constructs thus removing unconjugated NA-MAb or biotinylated intermediates that might interfere with subsequent targeting studies. The physical-chemical properties of the MAb-CNTs will also be characterized to determine particle size using TEM and atomic force microscopy (AFM).**

I. **Analysis of noncovalent MAb-CNT conjugates.**

The UV-Vis-NIR spectra of the MAb-CNT conjugates displayed the same metallic and semi-conducting CNT types as observed for the B-CNTs, indicating that the optical properties of the CNTs were not affected by the coupling (**Fig. 3a**), and the characteristic CNT resonances displayed in the Raman spectra of the MAb-CNTs again confirmed the presence of CNTs in the sample (**Fig**. **3b**).

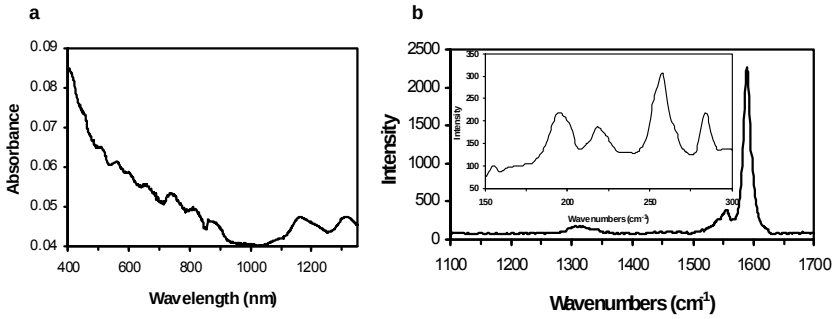

Figure 3. Optical properties of CNTs following coupling with MAbs. *(a)* UV-Vis-NIR spectra of RFB4-CNTs show the same metallic and semi-conducting CNT types as observed for the B-CNTs, indicating the retention of the optical properties of CNTs following the coupling with RFB4-NA. *(b)* Raman spectra of RFB4-CNTs show an intense G band (~1590 cm^{-1}) as the B-CNTs, indicating the presence of CNTs in the conjugate. The spectra are representative of three independent experiments.

II. **Analysis of covalent MAb-CNT conjugates.**

For AFM analysis, the samples were transferred into deionized water. **Figure 4a** shows a representative image of the CNTs after attaching them to RFB4. The images indicate a minimal amount of protein cross-linking that usually generates bundling of the CNTs. After attachment of RFB4, the diameter of the nanotubes increased from ~ 5 nm to ~16 nm (**Fig 4a, bottom panel**). The AFM images confirm the formation of the RFB4-CNT conjugate, although the nature of the linkage could be covalent and/or non-covalent. In order to confirm that the linkage was covalent, the MAb-CNTs were dispersed in sodium dodecylsulfate (SDS) and electrophoresed on a 7.5% polycrylamide gel electrophoresis (PAGE) under nonreducing conditions. The control sample contained a mixture of equivalent amounts of CNTs and MAb. As shown in **Fig. 4b**, no IgG was detected in the RFB4-CNT samples, demonstrating that the CNT-bound IgG remained in the loading well attached to CNTs. In contrast, a MAb band was detected in the "mixture" control. Taken together, these data indicate that the linkage between the MAbs and the CNTs was covalent.

We next determined if the optical properties and structure of the CNTs were affected by the covalent coupling. Pertinent to their use in photothermal therapy, the UV-Vis-NIR spectrum indicated that CNTs preserve their absorption in the NIR region **(Fig. 4c).** The resonant Raman scattering analysis indicates the quality of CNTs in the conjugate (**Fig. 4d**). Indeed, the RFB4-CNT conjugate exhibited the characteristic G band at ~1590 cm^{-1} derived from graphitic carbons. The high intensity of the G-band, assigned to the tangential mode of the graphene sheet,

compared with the D-band (~1370 cm^{-1}), ascribed to the Raman mode of the amorphous carbon, indicated the high purity of the sample.

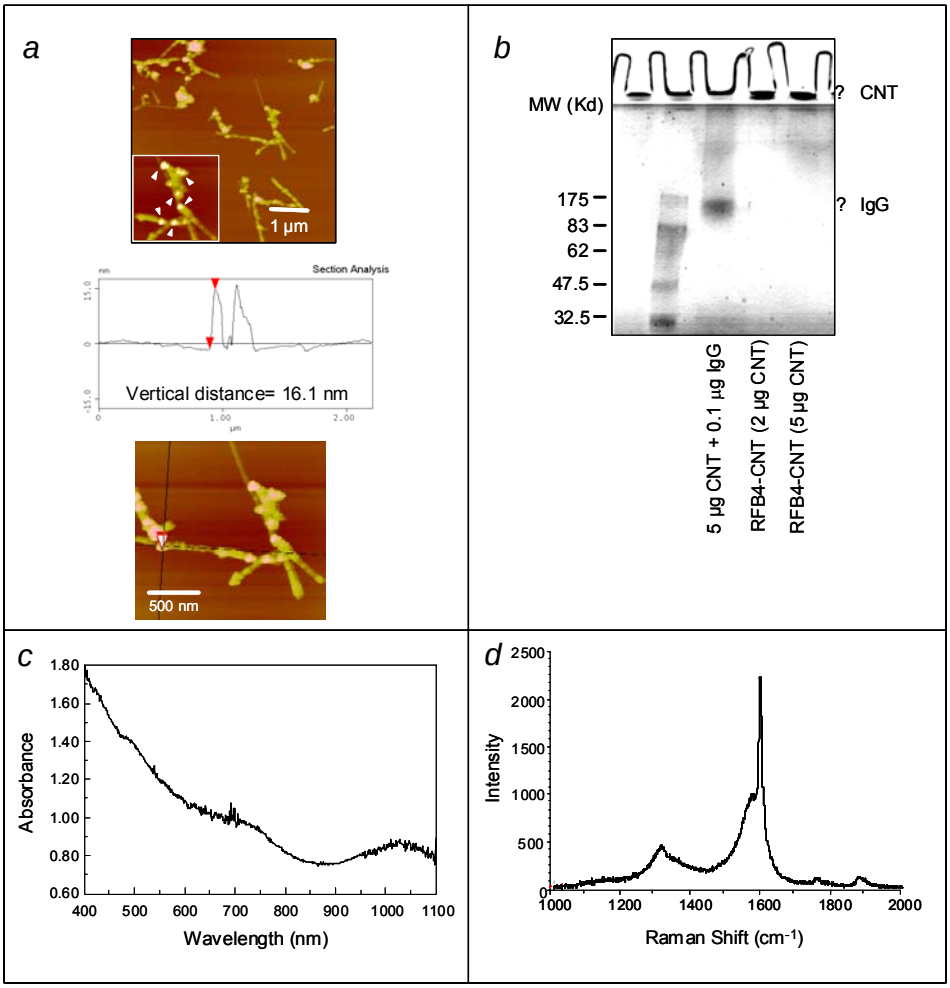

Figure 4. Physical and optical properties of RFB4-CNTs. *(a)* AFM image indicating the attachment of MAbs to CNTs. The enlarged inset shows where the MAbs are attached to the CNTs (arrowheads). The diameter of a coated region (~16 nm) is determined by AFM height analysis (*bottom panel*). This AFM image is representative of AFM images acquired from two unique MAb-CNT dispersions. *(b)* Stability of RFB4-CNTs. Purified RFB4-CNTs or a mixture of carboxylated CNTs and RFB4 (control) were subjected to SDS-PAGE. Samples containing 3 or 5 µg CNTs were loaded on the gel. The stacking gel shows the accumulation of CNTs whereas dissociated IgG migrated into the gel. The presence of dissociated protein was detected by staining with SimplyBlue SafeStain. *(c)* UV-Vis-NIR spectrum of RFB4-CNTs. *(d)* Raman spectrum of the carboxylated CNTs after covalent coupling of MAb. G band at ~1590 cm^{-1} is the characteristic Raman signal for CNTs. One representative experiment of three is shown in each panel.

Relationship to the work of others: The use of biotinylated phospholipids to non-covalently coat and disperse CNTs has the advantage of not disrupting the electronic structure of the CNTs. However, there is a potential limiting factor in using these CNTs in animals because non-covalently attached lipid material might be displaced by other macromolecules in biological fluids, resulting in the removal of the targeting moiety (4). The chemical and binding stability of the MAb-CNT conjugates as well as their stability in serum are important to establish before using them *in vivo*. For this reason, we tested an alternative strategy where the targeting molecule was covalently coupled to the CNTs. In order to do this, we used the carboxylic acid groups on chemically oxidized CNTs, which have the advantage of well-described chemistry (8-11). A potential disadvantage is that covalent modification of

CNTs may interfere with the electronic and optical properties of the CNTs. However, previous reports (12) indicated that water-soluble, mildly carboxylic acid-modified CNTs obtained by oxidative pretreatments retain their van Hove singularities which are critical for the absorption of NIR light. Previous reports have demonstrated that an anti-CD20 MAb covalently coupled to CNTs retained both linkage stability and specific targeting (13). These conjugates were used to deliver radionuclides to tumor cells *in vivo* and not for their ability to convert NIR light to heat, Since the chemistry of MAb attachment involved a sidewall ylide cycloaddition followed by 2-(4-isothiocyanatobenzyl)-1, 4,7,10-tetraazacyclododecane-1,4,7,10-tetraacetic (DOTA) and succiminidyl-4-(N-maleimidomethyl)cyclohexane-1-carboxy-(6-amidocaproate rather than direct attachment to terminal carboxyl groups, the photothermal property of the CNTs might have been compromised. Indeed, one of the major concerns with the covalent attachment of targeting ligands is that chemical stability can increase at the expense of photothermal efficacy due to the defects in the sp^2 hybridization of the CNTs induced by chemical functionalization. It has been noted that the Raman profile and NIR absorption of CNTs are significantly affected by their covalent modification (14). However, we found that chemical coupling of the MAb to CNT did not destroy the optical properties critical for the conversion of NIR light into heat.

Task 3. <u>To test targeting of MAb-CNTs to cells *in vitro*.</u>

I. **Specific binding of noncovalent MAb-CNT conjugates.**

The ability of the MAb-CNT conjugates to bind to antigen-positive but not antigen- negative target cells was assessed by flow cytometry. The components of the cell-bound MAb-CNT were detected using fluorescein-isothiocyanate-labeled goat anti-mouse Ig (FITC-GAMIg) (which reacts with mouse MAb) and phycoerythrin-labeled streptavidin (PE-SA) (which reacts with biotin), respectively. We found that RFB4-CNT and RFB4 (positive control) bound equally well to Daudi cells whereas RFT5-CNT (negative control) bound poorly ($p< 0.001$) (**Fig. 5a**). Conversely, RFT5-CNT and RFT5 bound equally well to $CD22^-CD25^+$ phytohemagglutinin (PHA)-activated peripheral blood mononuclear cells (PBMCs) (95% $CD25^+$ cells), whereas the negative control conjugate, RFB4-CNT, did not ($p < 0.002$) (**Fig. 5b).** These results demonstrate that the coupling of the MAbs to CNTs does not alter their MAb-binding activity and that the MAb-CNTs bind to antigen- expressing cells as specifically as the uncoupled MAbs.

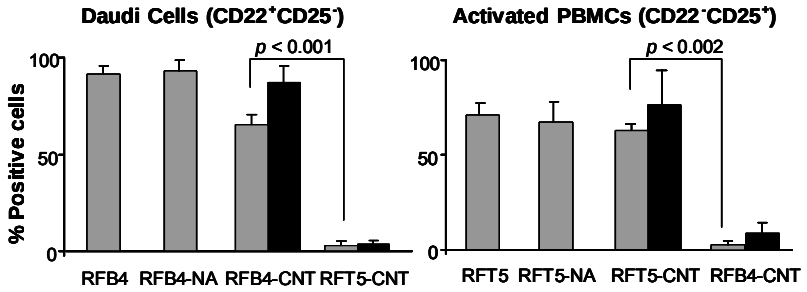

Figure 5. Binding of MAb-CNTs to target cells. The specific binding of RFB4-CNT to Daudi cells using RFT5-CNT as a negative control and the specific binding of RFT5-CNT to activated PBMCs (>95% T cells) using RFB4-CNT as negative control. A million cells were incubated with saturating concentrations of RFB4-CNT or RFT5-CNT and then incubated with either FITC-GAMIg to detect the MAb moiety or with PE-SA to detect the B-CNT moiety and analyzed by flow-cytometry.

II. **Specific binding of the covalent MAb-CNT conjugates.**

We determined the ability of these MAb-CNT conjugates to bind to $antigen^+$ but not $antigen^-$ target cells using flow cytometry. The cell-bound MAb-CNTs were detected using FITC-GAMIg. We found that RFB4-CNTs bound well to Daudi cells whereas the RFT5-CNTs (negative control) bound poorly (**Fig. 6a and b)**. Conversely, RFT5-CNTs and RFT5 bound equally well to $CD22^-CD25^+$ PHA-activated PBMCs (95% $CD25^+$ cells), whereas the negative

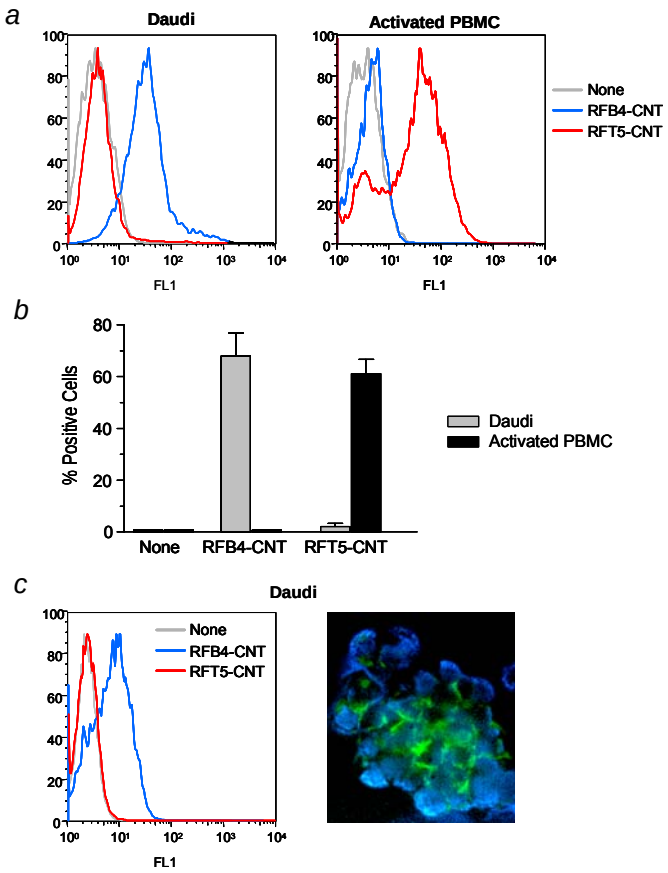

Figure 6. Specific binding of MAb-CNTs to target cells. *(a)* Daudi cells or PHA-activated human PBMCs were stained with either RFB4-CNTs or RFT5-CNTs (1 µg CNT) followed by FITC-GAMIg and cells were analyzed by flow cytometry. Histograms showing the staining with RFB4-CNTs (blue line) and RFT5-CNTs (red line) are overlaid on the ones corresponding to unstained cells (grey line) in each panel. *(b)* The results of three independent binding experiments are presented as means of % positive cells ± SD. The binding of MAb-CNTs to target *vs.* non-target cells was highly specific ($p<0.01$) *(c)* The binding of RFB4-CNTs to Daudi cells was confirmed by direct fluorescence using CNTs co-conjugated to RFB4 and EGFP. Cell binding was revealed by flow-cytometry *(left panel)* and fluorescence microscopy *(right panel)*.

control conjugate, RFB4-CNT, did not **(Fig. 6a and b)**. Additional experiments using non-activated, carboxyl-functionalized CNTs incubated with targeting antibody (control) indicated no detectable binding to cells (data not shown). This indicates that CNTs are free of adsorbed MAb. Taken together, these results demonstrate that the MAb-CNTs bind specifically to antigen- expressing cells. The binding to target cells was confirmed by flow cytometric analysis of the CNTs co-coupled to targeting MAb and EGFP **(Fig 6c, left panel)** and fluorescence microscopy (**Fig 6c, right panel).** The extensive binding and receptor cross-linking was confirmed by the massive homotypic adhesion of cells **(Fig 6c, right panel).**

The stability of the MAb-CNT conjugate was established by incubating RFB4-CNTs (1 µg CNTs) in 500 µl mouse serum at 37°C for up to 24 h. At the end of incubation, the RFB4-CNTs were recovered by centrifugation and then tested for their ability to bind to $CD22^+$ Daudi cells, using RFT5-CNT as negative control. As shown in **Figure 7**, we found that their binding was not diminished.

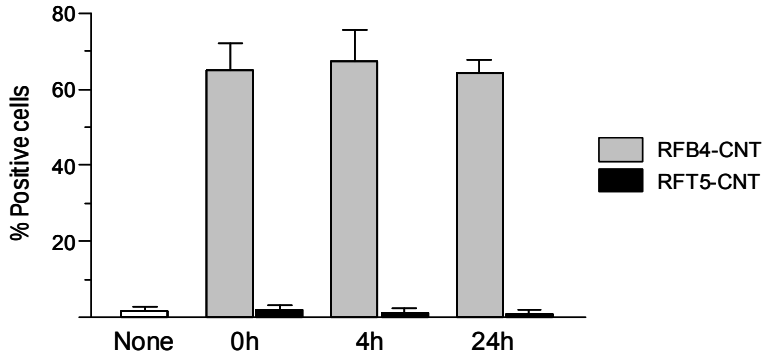

Figure 7. Binding stability of RFB4-CNTs. The stability of the RFB4-CNTs *in vitro* was determined by incubating them (1 μg CNT) in mouse serum at 37°C for 0, 4 and 24 h. At each time point, the RFB4-CNTs were recovered by centrifugation, washed with PBS and incubated with Daudi cells and the positive binding detected by flow-cytometry. Data represent mean ± S.D. of at least three independent experiments.

Relationship to the work of others: The targeting of CNTs to tumor cells can be accomplished by coating them with cell-binding ligands such as peptides or MAbs (1-3,15,16). Several studies have reported that the targeting of such CNTs is "specific" (1-3,13,15,16) but no study has used both a control ligand and a control cell to convincingly demonstrate ligand-specific thermal ablation of tumors cells with CNTs. In our study we provided clear evidence of specific binding to target cells with both types of MAb-CNTs.

Task 4. To assess the thermal ablation of the tumor cells in the model cell systems upon exposure to NIR light or RF waves.

I. **Thermal ablation of target cells by noncovalent MAb-CNT conjugates upon exposure to NIR.**
Having demonstrated that the MAb-CNT conjugates retained the binding activity of the MAb and the optical properties of the CNTs, we next determined whether cells targeted by the MAb-CNTs could be thermally ablated following exposure to NIR light. Cells were incubated with the MAb-CNTs in PBS, washed 3 times with PBS and then dispensed into 96-well plates in cell culture media. The cells in the plate were exposed to an 808 nm laser (5 W/cm^2) for 7 min and pulsed for the next 12 h with 1 μCi [^{3}H]-Thymidine to assess cell viability. As shown in **Fig. 8a**, as compared to treatment with the non-binding RFT5-CNTs, the viability of the RFB4-CNT-treated Daudi cells was significantly reduced following exposure to NIR light ($p<0.0001$). Conversely, when activated PBMCs were used as target cells, RFT5-CNT, but not RFB4-CNT, killed the cells following exposure to NIR light ($p<0.0001$) (**Fig. 8b).** These experiments demonstrate that the binding of the MAb-CNTs to their respective antigen-positive target cells leads to their specific ablation following exposure to NIR light.

Thermal ablation of target cells by covalent MAb-CNT conjugates upon exposure to NIR.

We tested whether cells targeted by the covalent MAb-CNTs could be thermally ablated following exposure to NIR light. Cells were incubated with the MAb-CNTs in PBS and after the excess unbound CNTs were removed, cells were suspended in culture medium and dispensed into 96-well plates. The cells in the plate were exposed to an 808 nm laser (9.5 W/cm^2) for 4 min and pulsed for the next 12 h with 1 μCi [^{3}H]-Thymidine to assess their proliferative capacity, which is our standard method to measure cell viability. As compared to the non-binding control RFT5-CNTs, the viability of the RFB4-CNT-treated Daudi cells was significantly ($p<0.01$) reduced following exposure to NIR light **(Fig 9a**). Conversely, when activated PBMCs were used as target cells, RFT5-CNTs, but not the control RFB4-CNTs, killed the cells following exposure to NIR light **(Fig. 9b).** The proliferation of cells treated with MAb-CNTs in the absence of NIR was significantly lower ($p<0.05$) than the proliferation of untreated cells. This may be due to an extensive cross-linking of the target antigen by the CNT-bound MAbs and subsequent signaling of growth arrest and/or apoptosis. This possibility is supported by the observation that cells undergo massive clustering, as shown in **Fig. 6c**. These experiments demonstrate that the binding of the MAb-CNTs to their target cells leads to

their specific ablation following exposure to NIR light and the overall inhibitory effect is further enhanced by receptor hyper-crosslinking.

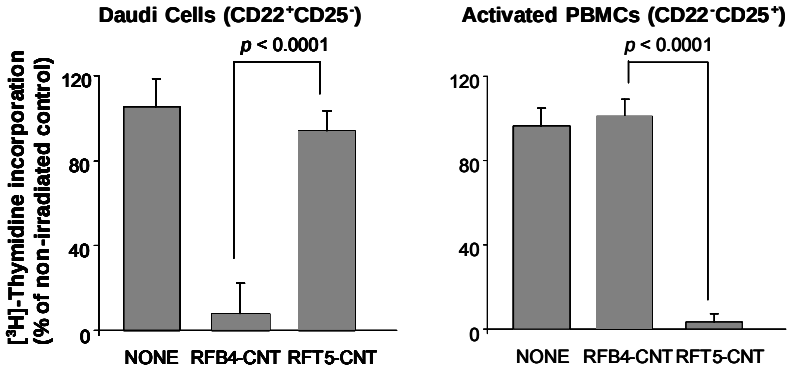

Figure 8. Ablation of MAB-CNT coated cells with NIR. The specific NIR-mediated thermal ablation of Daudi cells by RFB4-CNT using RFT5-CNT as negative control and of activated PBMCs (>95% T cells) by RFT5-CNT using RFB4-CNT as negative control. Cells (10^6) were incubated with saturating concentrations of RFB4-CNT or RFT5-CNT, wash out the excess and then dispensed into 96-well plates (10^5 cells/well). The cells were exposed for 7 min to 808 nm NIR light (5 W/cm^2), pulsed with 1μCi [^{3}H]-Thymidine and harvested 12 h later. The incorporated radioactivity was measured by liquid scintillation counting from triplicate samples. The percentage of radioactivity incorporated by each sample was calculated relative to corresponding non-irradiated sample. Data represent mean ± S.D. of at least three independent experiments. *P*-values were calculated utilizing paired, two-tail distribution Student's *t*-test.

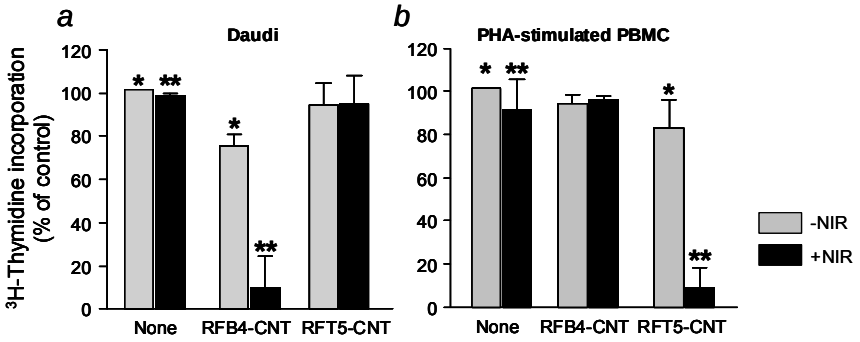

Figure 9. Specific killing of target cells by MAb-CNTs following exposure to NIR light. A million cells were incubated with MAb-CNTs containing 3 μg CNTs in PBS for 15 min at 4°C. Cells were washed three times with ice-cold PBS, and then 10^5 cells were dispensed in triplicate wells in a 96-well plate in 200 μl complete medium. The cells were exposed to continuous NIR light for 4 min at 9.5 W/cm^2. Cell death was assessed by pulsing the cells for the next 12 h with 1 μCi [^{3}H]-Thymidine/well and the incorporated radioactivity was measured by liquid scintillation counting. The incorporated radioactivity for each sample was calculated relative to the corresponding non-irradiated samples. *(a)* The specific killing of Daudi cells by RFB4-CNTs using RFT5-CNTs as the negative control. *(b)* The specific killing of activated PBMCs (>95% T cells) by RFT5-CNTs using RFB4-CNTs as the negative control (*, $p< 0.01$; **, $p< 0.05$). Data represent mean ± S.D. of at least three independent experiments.

Relationship to the work of others: The use of NIR-resonant nanostructures, including gold nanoshells and CNTs, to thermally ablate cancer cells is being explored by several groups (1,2,17-20). The use of NIR light in the 700-1100 nm range for the induction of hyperthermia is particularly attractive because living tissues do not strongly absorb in this range (16). The critical aspect for selective CNT-mediated thermal ablation of cells is to stably attach targeting moieties that will not interfere with the optical properties of the CNTs and yet retain targeting specificity.

We found that CNTs attached to MAbs by covalent bonds could thermally ablate target cells with the same efficiency as CNTs attached to MAbs by non-covalent bonds. CNT conjugates described in this study are biocompatible with cells *in vitro*. However, cells cultured with target-specific covalent MAb-CNTs did not proliferate as well due to receptor-mediated signaling of cell cycle arrest and/or cell death. This has been observed previously using cross-linking MAbs specific for different B cell surface markers and is therefore not surprising (21, 22).

Task 5. <u>To determine the biodistribution and pharmacokinetics of MAb-CNTs in mice with and without tumors.</u>

The final objective if this work is to determine the biodistribution and pharmacokinetics of these conjugates in experimental mice. The model system we will use is SCID mice bearing s.c human B lymphoma. However, within the year allotted to this proposal there was insufficient time to finalize this task. The data from these studies will provide key information for the future design of local and systemic ablation of tumors in mice.

As a preliminary step for determining the biodistribution of the CNTs, we set up a sensitive technique to determine the concentration of CNTs in homogenates of various mouse organs. We chose to use the intrinsic CNT property (e.g. 1590 cm^{-1} Raman G-band signature) for tracking rather than using radiolabelled CNTs, which would alter the specific optical properties and stability of the CNT dispersions. The homogenates were placed in glass-bottom dishes and measured by Raman spectroscopy. The G band peak area was integrated from 1570 cm^{-1} to 1620 cm^{-1} and averaged for multiple spectra and then plotted against the concentrations of CNTs. A typical Raman shift plot for serial dilutions of CNTs in PBS is shown in **Fig. 10a** and the standard curve in **Fig. 10b**. Similar standard curves were generated using homogenates of mouse organs spiked with CNTs. To this end mice were sacrificed and perfused with saline. Organs were collected, lyophilized and then mechanically homogenized after digestion with collagenase followed by the addition of sodium dodecyl sulafate (SDS). Then, known amounts of CNTs were added to the tissue homogenate. Two such standard curves generated for liver and spleen as shown in **Fig. 10c and d**.

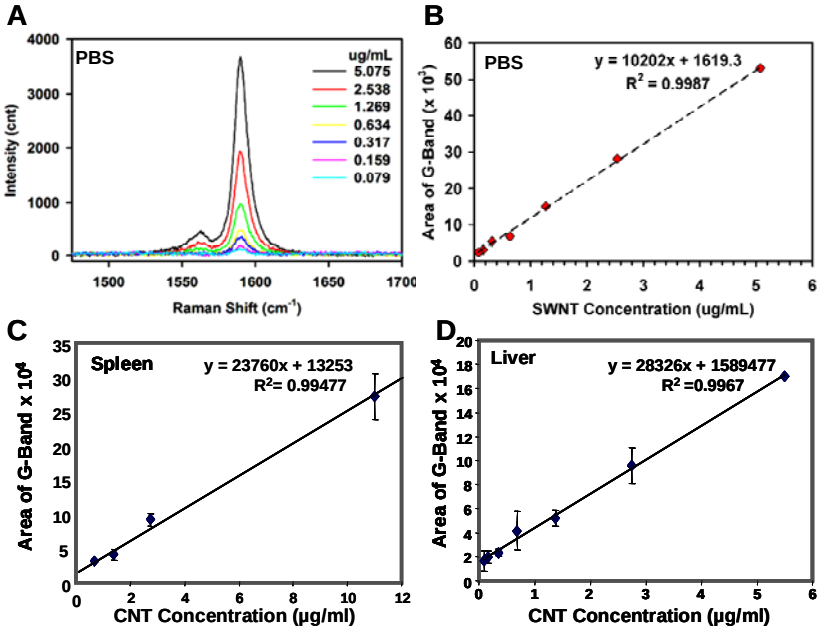

Figure 10. Standard Raman calibration curve of CNT solutions. *(a)* A typical Raman spectrum of CNT in PBS at different concentrations after subtracting background. *(b)* Standard curve for CNT concentration (G-band region intensity *vs.* CNT concentration) in PBS or *(c* and *d)* in lyophilized mouse liver and spleen tissue powder suspended in surfactant solutions.

Relationship to the work of others: Our detection method takes advantage of the inherent Raman peak of the graphite structure in CNTs to quantitate them in different excised tissue samples without adding radioactive isotopes that could potentially influence their biodistribution. In addition, the modification of CNTs with both a DOTA (1,4,7,10-tetraazacyclododecane-1,4,7,10- tetraacetic acid) metal chelator is difficult to prepare; and the radiolabeling procedure can be costly and time-consuming involving unnecessary radiation exposure. Our Raman imaging method is consistent with previous reports (5).

Having demonstrated excellent specificity of both targeting and thermal ablation *in vitro*, we are currently evaluating the pharmacokinetics, biodistribution, toxicity and activity of these MAb-CNT constructs *in vivo*.

KEY RESEARCH ACCOMPLISHMENTS:

CNTs attached to MAbs for targeting and photothermal ablation of tumor cells are:

- Well-dispersed and retained their optical properties;
- The MAb-CNT conjugates are chemically stable
- The conjugates bound specifically to target cells and binding remained specific even after the MAb-CNTs were incubated in mouse serum;
- Specifically targeted cells can be thermally ablated following exposure to NIR light.

REPORTABLE OUTCOMES:

Papers:

1. Chakravarty P, Marches R, Zimmerman NS, Swafford AD, Bajaj P, Musselman IH, Pantano P, Draper RK, Vitetta ES. Thermal ablation of tumor cells with antibody-functionalized single-walled carbon nanotubes. *Proc. Natl. Acad. Sci. USA*. 105: 8697-702, 2008.

2. Marches R, Chakravarty P, Musselman IH, Azad, R, Draper RK, Vitetta ES. Selective thermal ablation of tumor cells using a monoclonal antibody covalently coupled to single-wall carbon nanotubes *(submitted to Int. J. Cancer)*.

3. Wang R, Mikoryak C, Chen E, Li S, Pantano P, Draper RK. A sensitive gel electrophoresis method to measure the concentration of single-walled carbon nanotubes *(submitted)*

Presentations:

1. Swafford AD, Chakravarty P, Dieckmann G, Draper RK, Musselman IH, Pantano P, Marches R, Vitetta ES. Isolation and analysis of MAb/Single-walled carbon nanotube complexes by ultracentrifugation in iodixanol. STARS presentation forum, UT Southwestern Medical Center, 2007.

Grants:

1. Texas Advanced Research (Biological Sciences) Program grant No. 009741-0005-2007 – Antibody-conjugated carbon nanotubes for selective photothermal ablation of human tumors (2007).
2. NIH R01 - Her2 targeted carbon nanotubes for photothermal ablation of breast tumors- *Application Number:* NIH R01 CA138813-01 (2008).

Ph.D. students:

1. Pavitra Chakravarty – Bioengineering, - UT Arlington. / UT Southwestern Medical Center

CONCLUSION:

The in vitro studies indicate a good selectivity of thermal ablation achieved with MAb-targeted CNTs under NIR light. The MAb-CNTs do not pose any inherent cytotoxic effect and are relatively stable in mouse serum. The covalent MAb-CNTs might present an advantage over the noncovalent ones for in vivo treatments in terms of stability/specificity. However, a final conclusion will be reached after the biodistribution, pharmacokinetics and animal toxicity tests.

REFERENCES:

1. Kam NW, O'Connell M, Wisdom JA, Dai H. Carbon nanotubes as multifunctional biological transporters and near-infrared agents for selective cancer cell destruction. *Proc Nat Acad Sci* 102: 11600-11605, 2005.
2. Shao N, Lu S, Wickstrom E, Panchapakesan B. Integrated molecular targeting of IGF1R and Her2 surface receptors and destruction of breast cancer cells using single wall carbon nanotubes. *Nanotechnol* 18: 315101-315109, 2007.
3. Welsher K, Liu Z, Daranciang D, Dai H. Selective probing and imaging of cells with single walled carbon nanotubes as near-infrared fluorescent molecules. *Nano Lett* 8: 586-590, 2008.
4. Cherukuri P, Gannon CJ, Leeuw TK, Schmidt HK, Smalley RE, Curley SA, Weisman RB. Mammalian pharmacokinetics of carbon nanotubes using intrinsic near-infrared fluorescence. *Proc Natl Acad Sci USA.* 103: 18882-18886, 2006.
5. Liu Z, Cai W, He L, Nakayama N, Chen K, Sun X, Chen X, Dai H. In vivo biodistribution and highly efficient tumor targeting of carbon nanotubes in mice. *Nat Nanotechnol.* 2007; 2: 47-52.
6. Schipper ML, Nakayama-Ratchford N, Davis CR, Kam NW, Chu P, Liu Z, Sun X, Dai H, Gambhir SS. A pilot toxicology study of single-walled carbon nanotubes in a small sample of mice. *Nat Nanotechnol.* 2008; 3: 216-221.
7. Sayes CM, Fortner JD, Guo W, Lyon D, Boyd AM, Ausman KD, Tao YJ, Sitharaman B, Wilson LJ, Hughes JB, West JL, Colvin VL. The differential cytotoxicity of water soluble fullerenes. *Nano Lett.* 2004; 4: 1881-1887.
8. Coleman KS, Azamian BR, Davis JJ, Bagshaw CB, Green MLH. Chemistry, biochemistry, and electrochemistry of single-walled carbon nanotubes. *Pap Am Chem S* 224: U420-U421, 2002.
9. Bianco A, Kostarelos K, Partidos CD, Prato M. Biomedical applications of functionalized carbon nanotubes. *Chem Commun.* 571-577, 2005.
10. Lin Y, Taylor S, Li HP, Fernando KAS, Qu LW, Wang W, Gu LR, Zhou B, Sun YP. Advances toward bioapplications of carbon nanotubes. *J Mater Chem.* 14: 527-541, 2004.
11. Huang W, Taylor S, Fu K, Lin Y, Zhang D, Hanks TW, Rao AM, Sun Y. Attaching proteins to carbon nanotubes *via* diimide-activated amidation. *Nano Lett.* 2: 311-314, 2002.
12. Zhao W, Song C, Pehrsson PE. Water-soluble and optically pH-sensitive single-walled carbon nanotubes from surface modification. *J Am Chem Soc.* 124: 12418-12419, 2002.
13. McDevitt MR, Chattopadhyay D, Kappel BJ, Jaggi JS, Schiffman SR, Antczak C, Njardarson JT, Brentjens R, Scheinberg DA. Tumor targeting with antibody-functionalized, radiolabeled carbon nanotubes. *J Nucl Med.* 48: 1180-1189, 2007.
14. Wang Y, Iqbal Z, Mitra S. Rapidly functionalized, water-dispersed carbon nanotubes at high concentration. *J Am Chem Soc.* 128: 95-99, 2006.
15. Liu Z, Sun X, Nakayama-Ratchford N, Dai H. Supramolecular chemistry on water-soluble carbon nanotubes for drug loading and delivery. *ACS Nano* 1: 50-56, 2007.
16. Weissleder R. A clearer vision for *in vivo* imaging. *Nature Biotechnol.* 19: 316-317, 2001.
17. Gobin AM, Lee MH, Halas NJ, James WD, Drezek RA, West JL. Near-infrared resonant nanoshells for combined optical imaging and photothermal cancer therapy. *Nano Lett.* 7: 1929-1934, 2007,
18. Loo C, Lowery A, Halas N, West J, Drezek R Immunotargeted nanoshells for integrated cancer imaging and therapy. *Nano Lett* 5: 709-711, 2005.
19. Huang X, El-Sayed IH, Qian W, El-Sayed MA. Cancer cell imaging and photothermal therapy in the near-infrared region by using gold nanorods. *J Am Chem Soc* 128: 2115-2120, 2006.
20. Hirsch LR, Stafford RJ, Bankson JA, Sershen SR, Rivera B, Price RE, Hazle JD, Halas NJ, West JL. Nanoshell-mediated near-infrared thermal therapy of tumors under magnetic resonance guidance. *Proc Natl Acad Sci USA.* 100: 13549-13554, 2003.

21. Ghetie MA, Picker LJ, Richardson JA, Tucker K, Uhr JW, Vitetta ES. Anti-CD19 inhibits the growth of human B-cell tumor lines in vitro and of Daudi cells in SCID mice by inducing cell cycle arrest. *Blood.* 1994; 83:1329-1336.

22. Marches R, Scheuermann RH, Uhr JW. Cancer dormancy: role of cyclin-dependent kinase inhibitors in induction of cell cycle arrest mediated via membrane IgM. *Cancer Res.* 1998; 58: 691-697.